Fractional Frequency Reuse in Ultra Dense Networks

Sinh Cong Lam*, Xuan Nam Tran†,

* Univeristy of Engineering and Technology, Vietnam National University - Hanoi,

† Advanced Wireless Communications Group, Le Quy Don Technical University, Vietnam,

Abstract

Ultra Dense Network (UDN) in which Base Stations (BSs) are deployed at an ultra high density is a promising network model of the future wireless generation. Due to ultra densification, reuse of frequency bands with a ultra high density is compulsory for this network. However, the research work on the deployment of frequency reuse technique such as Fractional Frequency Reuse (FFR) on UDNs has not been well-investigated. This paper focuses on modeling and performance analysis of a general FFR model in UDNs. Instead of assuming that there are are two user groups in each cell, the associated users in this paper are classified into N groups in which each group is served by a specific power level. The paper introduces a simple approach to obtain the coverage probability of a typical user in the case of a general path loss model. In the case of stretch path loss model for UDN, the approximated expression of user coverage probability is derived. Throughout the analytical and simulation results, there important conclusions are stated: *(i)* the user coverage probability increases to a peak before passing a decline when the density of BSs increases; *(ii)* an increase in BS transmission power may decrease the user performance; *(iii)* a higher number of user groups can improve the user performance.

Index Terms

Ultra Dense Network, Fractional Frequency Reuse, Poisson Point Process, Coverage Probability

I. Introduction

In recent years, the number of networked devices and the mobile traffic have risen critically. According to Cisco report [1], the number of networked devices in 2023 will reach 29.3 billions which is about 3 times greater than the world population. This will make the mobile data traffic increase by 8 times

in next few years. The explosive growth has encouraged the development of the sixth generation (6G) mobile networks to provide the ultra-high data rate, ultra-low latency, ultra-large number of connections as well as ultra-wide coverage area [2], [3]. To meet the requirements of 6G networks, Ultra Dense Networks (UDNs) in which the distance between two adjacent Base Stations (BSs) is around 10m has been introduced as a promising solution [4], [5]. The millimeter wave is recognized as the ideal frequency bands for UDNs.

However, the deployment of BSs with an ultra-high dense introduces new challenges. Specifically, the power loss of the transmitted signal in UDNs should be carefully investigated since the mmWave is extremely sensitive to transmission environment. Moreover, the interference between cells can not be ignored when the BSs are very close together. Therefore, a large number of research works have been conducted to investigate the UDNs performance analysis through path loss modeling and intercell interference coordination technique.

The performance of wireless systems strongly depends on the power loss of the radio signal. In order to analyze the network performance, the path loss model should be studied first. The multi-slope path loss model in which the signal can experience more than one path loss exponents was widely studied [6], [7], [8], [9]. For each slope, the power loss follows the conventional model which is formulated as $Loss = r^{-\alpha}$, in which r and α are the horizontal distance and the path loss exponent. The authors based on the probability of Line-of-Sight (LoS) and non-Line-of-Sight (nLoS) to compute the power loss over the transmission link. The coverage probability and spectrum efficiency were analyzed. The impacts of density of BSs and their heights were examined [10], [11], [12]. Other related works modeled the power loss as a exponential function of the distance such as [13], [14]. Recently, the stretched path loss model was introduced in Reference [15]. In this model, the path power loss over a distance r is determined as αr^{β} in which α and β are turnable parameters. Through experimental measurements, the author proved that the stretched path loss is more suitable for UDNs than previous models in the literature. Thus, we utilize this model to analyze the UDNs.

Frequency Reuse technique is a popular technique in wireless communications, in which two cells in a cellular system can use the same frequency band. The demand for reuse of frequencies became more necessary in the 4G systems since these system requires much more BSs to cover the services area than its previous generations. Thus, the Frequency Reuse technique has been improved to allow two adjacent BSs transmit on the same frequency band at the same time. Currently, this technique is known

as Fractional Frequency Reuse (FFR). The ideal of FFR is to divide the associated users and allocated frequency resources into 2 groups respectively so that each group of users is served by a particular group of frequency resources. By this way, the intercell interference can be minimized and the user performance can be improved. Althrough Fractional Frequency Reuse (FFR) has well-investigated for 4G systems, the deployment of this technique for future cellular network systems such as 6G is being at the early stage[16], [17], [18], [19], [20], [21]. The authors in [16], [22] discussed about the challenges and approaches of FFR utilization in the future cellular systems. The effects of FFR algorithm on network performance were discussed in [19]. In this work, the optimal frequency reuse factor was derived to optimize energy and spectral efficiency. The author in [21] introduced an approach to achieve load-balancing between macro BSs and small BSs. Although these works derived important concepts about FFR algorithm techniques for the future mobile systems, the classification of users into groups has not been well-discussed. The author in [20] discussed about the user classification. However, this work only performed simulation with the mmWave at 26-GHz band. Moreover, in all works discussed above, the two-phase operation of FFR algorithm has not been studied. This motives us to model and examine the performance of FFR algorithm in UDNs.

The performance analysis of FFR for regular cellular networks with low densities of BSs has been conducted in some interesting works in the literature. Reference [23] introduced an analytical approach and important initial results regarding to the effects of FFR on the cellular networks. In our work [24], the uplink performance with power control was considered. The closed-form expressions of performance metrics were given by utilizing Gaussian Quadrature. Recently, the author in [25], [26] presented fully closed-form expression. However, these work only studied regular path loss model in which the received power over a distance of r is $Pr^{-\alpha}$ (P is the transmission power). In the case of UDN, as discussed in previous paragraph, this path loss is no longer suitable and should be replaced by stretch path loss model αr^{β}. With the deployment of stretch path loss model, the kernel integral of user performance metric expressions became more complicated [15], [27]. Thus, the approaches in [24], [25], [26] are no longer applicable and the closed-form expressions were only found in the form of Polylogarithm function when $2/\beta$ is an integer number. In this paper, we bases on the Taylor expansions to obtain the simple form of the performance metrics before utilizing confluent hypergeometric function and Gauss - Laguerre quadrature to derive their closed-form expressions for all case of β. In the case of $2/\beta$, the closed-form expressions degrade into much more simple forms which does not rely on confluent hypergeometric function.

Moreover, the works in the literature only discussed FFR with two user groups and two power levels which is equivalent to FFR with the reuse factor of 3. In our recent works [28], a general FFR algorithm with N user group was introduced for regular cellular networks with low density of BSs and path loss model $r^{-\alpha}$. However, in these type of networks, the downlink SINR does not vary significantly over distance [29]. Thus, an increase in number of user groups N did not bring any benefit to the user performance as shown in [28]. In contrast, mmWave experiences fast attenuation over distances, the downlink SINR of user in UDNs usually varies over a large range. Thus, the FFR with two user groups may not be suitable for UDNs. This paper indicates that the user coverage probability is significantly improved when the number of user groups increases from 2 to 3 while the total power consumption remains unchanged.

Generally, compared to the aforementioned works in the literature, the contributions of this work are summarized as follows

- We investigate the general model of FFR for UDNs in which the users are classified into N groups. Each group of users is served by a appropriate power level. Thus, N power levels are utilized in this system model.
- We introduce an other approach to obtain the simple form of user coverage probability expression under a general path loss model. In the case of stretch model, we derive its closed-form expression by following confluent hypergeometric function and Gauss - Laguerre quadrature.
- Two interesting findings are found in this work. Firstly, the user coverage probability reaches a peak before passing a decline when the density of BSs increases. Secondly, an increase in transmission power may result in a decline in user coverage probability.
- The analytical results indicates that the user coverage probability can increase upto 13.9% when the number of user groups rises from 2 to 3 and the total power of the BSs is kept constant.

II. System model

This paper studies single tier UDNs in which BSs are distributed according to a spatial Poison Point Process (PPP) with mean λ (BS/km^2). Denote θ is the set of BSs in the networks.

It is supposed that all the signals traveling within the network area experiencing the same path loss model and Rayleigh fading with PDF $f(\gamma) = \exp(-\gamma)$. Denote L_r is the received power over a distance of r when the transmit power is 1. L_r can be called as power loss or path loss over a distance r. L_r is a decreasing function.

The user usually prefers a connection to BS n with the strongest average received signal strength. For example, the user associates with a BS at a distance if its average received signal strength $PL_r > PL(r_k)$ $\forall k \in \theta \backslash n$ or $r < r_k, \forall k \in \theta \backslash n$. Thus, it is state that in the case of the same path loss model, the BS with the highest average received signal of a user is the nearest BS of that user. The PDF and CDF of r are respectively given by

$$f(r) = 2\pi\lambda \exp(-\pi\lambda r^2) \tag{1}$$

$$\text{and } F(r) = 1 - \exp(-\pi\lambda r^2) \tag{2}$$

For the utilization of FFR, each BS classifies its associated users into N groups by $N + 1$ SINR thresholds, denoted by T_0, T_2,....,T_N. It is assumed that $T_0 \leq T_2 \leq .... \leq T_N$. Meanwhile T_0 and T_N are lower and upper bounds of SINR respectively, other values of T_1, T_2, ... ,T_{N-1} can be chosen appropriately for particular purposes such as user performance optimization or minimize power consumption. Each group of users are served by a specific power level. Thus, each BS utilizes N power levels such as P_1, P_2,...,P_N ($P_1 \geq P_2 \geq ... \geq P_N$). The lowest power level P_N is set at the transmit power P on the control channel, $P_N = P$. The operation of FFR can be modeled as two consecutive phases which are called establishment phase and communication phase.

A. Establishment phase

The total interference power on a single control channel during the establishment phase is given by

$$I_o = \sum_{j \in \theta} P_N g_j^{(o)} L_{r_j} \tag{3}$$

in which $g_j^{(o)}$ is the power gain of the channel from the user to interfering BS j.

Thus, the SINR is obtained by

$$SINR^{(o)}(r) = \frac{P_N g^{(o)} L_r}{I_o + \sigma^2} \tag{4}$$

The event that a user is assigned into Group n is defined as

$$T_{n-1} < SINR^{(o)}(r) < T_n \tag{5}$$

and the corresponding probability is given by

$$\mathcal{P}_{An}(r) = \mathbb{P}\left[T_{n-1} < SINR^{(o)}(r) < T_n\right] \tag{6}$$

Substituting Equation 4 into Equation 6, we obtain

$$\begin{aligned}\mathcal{P}_{An}(r) =& \mathbb{P}\left[T_{n-1} < \frac{P_N g^{(o)} L_r}{I_o + \sigma^2} < T_n \middle| r\right] \\ =& \mathbb{P}\left[T_{n-1}\frac{I_o + \sigma^2}{P_N L_r} < g^{(o)} < T_n \frac{I_o + \sigma^2}{P_N L_r}\middle| r\right]\end{aligned} \tag{7}$$

The probability above can be obtained from Appendix A with $\hat{T} = 0$. Hence, the association probability $\mathcal{P}_{An}(r)$ is given by

$$\mathcal{P}_{An}(r) = s_{n-1}\exp\left(-\frac{2\pi\lambda}{T_{n-1}}\upsilon(T_{n-1})\right) - s_n \exp\left(-\frac{2\pi\lambda}{T_n}\upsilon(T_n)\right) \tag{8}$$

in which M is an integer and is selected so that the Taylor series in Equation 34 converges. For sufficient computation, $M = 10$ is selected in this paper.

$$\upsilon(x) = \begin{cases} \left(\begin{array}{l} \sum_{m=1}^{M}(-1)^{m-1}L_r^{m-1}x^{2-m}\int_r^{L_{\frac{L_r}{x}}^{-1}} r_j L_{r_j}^{1-m} dr_j \\ +\sum_{m=0}^{M}(-1)^m x_n^{m+2} L_r^{-1-m}\int_{L_{\frac{L_r}{x}}^{-1}}^{\infty} r_j L_{r_j}^{m+1} dr_j \end{array}\right) & for \quad x > 1 \\ \sum_{m=0}^{M}(-1)^m x^{m+2} L_r^{-1-m}\int_r^{\infty} L_{r_j}^{m+1} r_j dr_j & for \quad x < 1 \end{cases} \tag{9}$$

and $\hat{s} = \exp\left(-\frac{1}{L(r)}\frac{\hat{T}}{\gamma_n}\right)$ and $s_n = \exp\left(-\frac{1}{L(r)}\frac{T_n}{\gamma_N}\right)$.

The association probability of the typical user in the network with Group n is obtained by

$$\mathcal{P}_{An} = 2\pi\lambda\int_0^{\infty}\left[s_{n-1}\exp\left(-\frac{2\pi\lambda}{T_{n-1}}\upsilon(T_{n-1})\right) - s_n\exp\left(-\frac{2\pi\lambda}{T_n}\upsilon(T_n)\right)\right] f(r)dr \tag{10}$$

B. Communication phase

With the employment of FFR, since the BS utilizes a higher power level to serve users with the lower received signal strength, Group n which contains of users with $T_{n-1} < SNR < T_n$ will be served by transmission power level P_n.

Due to sharing the RBs between cells, each user experiences ICI from all neighbouring cells. These interfering cells can be classified into N groups in which interfering group k transmits at a power level of P_k. Let λ_k is the density of interfering BSs in Group k. Then $\bigcap_{k=1}^{N}\theta_k = \theta$ and $\sum_{k=1}^{N}\lambda_k = \lambda$

The interference power from BSs in Group k is determined by

$$I_k = P_k \sum_{j \in \theta_k} g_j L_{r_j} \tag{11}$$

in which r_j and g_j is the distance and channel power gain from the user to its interfering BS j in Group k

The total ICI power at the typical user is given by

$$I = \sum_{k=1}^{N} P_k \sum_{j \in \theta_k} g_j L_{r_j} \tag{12}$$

The downlink SINR of a user in Group n during the communication phase is given by

$$SINR_n(r) = \frac{P_n g L_r}{\sum_{k=1}^{N} P_k \sum_{j \in \theta_k} g_j L_{r_j} + \sigma^2} \tag{13}$$

in which g and r is the channel power gain and the distance from the user to its serving BS.

III. Performance Evaluation

A. Definition metrics

a) Coverage Probability of a user in Group n : The user in Group n is under network coverage if

1) Its downlink SNR during establishment phase satisfies Inequality 5
2) Then, its downlink SINR during communication phase is greater than the pre-defined coverage threshold $\hat{T}$

Therefore, the coverage probability of the user in Group n formulated as the following conditional probability

$$\mathcal{P}_n(\hat{T}) = \mathbb{P}\left(SINR_n(r) > \hat{T} | T_{n-1} < SINR^{(o)}(r) < T_n\right) \tag{14}$$

in which

- $T_{n-1} < SINR^{(o)}(r) < T_n$ is the event that the user associates with Group n
- $SINR_n(r) > \hat{T}$ is to ensure that the received SINR of the user during communication phase is greater than the required SINR for successful data transmission.

The coverage probability definition in Equation 14 covers other definitions in related works in the literature. For example,

- The definition in References [30], [31] for single group of users and can be obtained by selecting $N = 1$, $T_0 = 0$ and $T_1 = \infty$.
- The definition in References [23], [32] for two groups of users corresponds to $N = 2$, $T_1 = 0$, $T_1 = T$ and $T_2 = \infty$.

Theorem 3.1: The coverage probability of the user in Group n in SINR-based model is given by

$$\mathcal{P}_n = \frac{2\pi\lambda \int_0^{\infty} \left[\begin{pmatrix} \hat{s}s_{n-1} \prod_{k=1}^{N} \exp\left[-\frac{2\pi\lambda_k}{\hat{T}\frac{\gamma_k}{\gamma_n} - T_{n-1}} \left(\upsilon\left(\hat{T}\frac{\gamma_k}{\gamma_n}\right) - \upsilon(T_{n-1}) \right) \right] \\ -\hat{s}s_n \prod_{k=1}^{N} \exp\left[\frac{2\pi\lambda_k}{\hat{T}\frac{\gamma_k}{\gamma_n} - T_n} \left(\upsilon\left(\hat{T}\frac{\gamma_k}{\gamma_n}\right) - \upsilon(T_n) \right) \right] \end{pmatrix} \right] f(r)dr}{2\pi\lambda \int_0^{\infty} \left[s_{n-1} \exp\left(-\frac{2\pi\lambda}{T_{n-1}} \upsilon(T_{n-1}) \right) - s_n \exp\left(-\frac{2\pi\lambda}{T_n} \upsilon(T_n) \right) \right] f(r)dr} \tag{15}$$

Proof: See Appendix A □

The expression of coverage probability P_n in Equation 15 can cover all related cases in the literature. For example, the results in [23] refers to N=2 and threshold $T_1 = 0, T_2 = T$ and $T_3 = \infty$. P_1 and P_2 corresponds to coverage probability of Cell-Center User and Cell-Edge User respectively.

Furthermore, this expression is much more simple than related previous expressions in the literature for $N \leq 2$ such as [23], [15]. Take the regular path loss model in which the path loss over a distance r and path loss exponent τ is $r^{-\tau}$ for example. The integral of $\upsilon(x)$ has a form of $\int_a^{\infty} y^{-z} dy$ $(z > 0)$ and can be computed easily.

b) Coverage probability of a typical user: The typical user that is located at a random position in the network can be assigned to any group. Thus, the coverage probability of the typical user is defined as

$$\mathcal{P}(\hat{T}) = \sum_{n=1}^{N} \mathbb{E}\left[\mathcal{P}_n(\hat{T}|r) \mathcal{P}_{An}(r) \right] \tag{16}$$

in which

- $\mathcal{P}_n(\hat{T}|r)$ is the coverage probability of the user at distance r from its serving BS.
- $\mathcal{P}_{An}(r)$ is the probability of that user to be assigned into Group n

Taking the expected value with respect to the variable r, the we get

$$\mathcal{P}(\hat{T}) = 2\pi \sum_{n=1}^{N} \lambda_n \int_0^{\infty} \mathbb{E}\left[\mathcal{P}_n(\hat{T}|r) \mathcal{P}_{An}(r) \right] \exp\left(-\pi\lambda r^2 \right) dr \tag{17}$$

Corollary 3.1: The coverage probability of the typical user is given by

$$\mathcal{P}(\hat{T}) = 2\pi \sum_{n=1}^{N} \lambda_n \int_0^{\infty} \left[\left(\begin{array}{c} \prod_{k=1}^{N} \hat{s} s_{n-1} \exp\left[-\frac{2\pi\lambda_k}{\hat{T}\frac{\gamma_k}{\gamma_n} - T_{n-1}} \left(\upsilon\left(\hat{T}\frac{\gamma_k}{\gamma_n} \right) - \upsilon(T_{n-1}) \right) \right] \\ - \prod_{k=1}^{N} \hat{s} s_n \exp\left[-\frac{2\pi\lambda_k}{\hat{T}\frac{\gamma_k}{\gamma_n} - T_n} \left(\upsilon\left(\hat{T}\frac{\gamma_k}{\gamma_n} \right) - \upsilon(T_n) \right) \right] \end{array} \right) \right] \exp(-\pi\lambda r^2) dr \tag{18}$$

Proof: The coverage probability of the typical user in Equation 16 is re-formulated as follows

$$\mathcal{P}(\hat{T}) = \sum_{k=1}^{N} \mathbb{E}\left[\mathbb{P}\left(SINR(r) > \hat{T} \middle| T_{n-1} < SINR^{(o)}(r) < T_n \right) \mathbb{P}\left(T_{n-1} < SINR^{(o)}(r) < T_n \right) \right] \tag{19}$$

$$= \sum_{k=1}^{N} \mathbb{E}\left[\mathbb{P}\left(SINR(r) > \hat{T}, T_{n-1} < SINR^{(o)}(r) < T_n \right) \right] \tag{20}$$

where (20) is obtained by following the Bayes rule.

Using the result of Appendix A, the desired result can be given. □

c) The power consumption: Since a user at a distance r from its serving BS is assigned to Group n and served by a power level of P_n with a probability of P_{An}, the power power consumption of a BS, which is utilized to serve the this user is

$$\overline{P}_n = P_n P_{An} \tag{21}$$

in which P_{An} is defined in Equation 8.

The power consumption of the BS uses to serve the typical user is obtained by

$$\overline{P} = \sum_{n=1}^{N} \int_0^{\infty} P_n P_{An} f(r) dr \tag{22}$$

IV. Approximated expressions for Stretched Path Loss Model

The path loss under stretch path loss model over a distance r is defined by $L_r = \exp(-\alpha r^{\beta})$ in which α and β are tunable parameters. While β represents the density of obstacles on the radio channel, α depends on characteristics of these obstacles. The inverse function of the path loss is $L^{-1}(x) = \left(-\frac{\log x}{\alpha}\right)^{1/\beta}$.

It is seen from Equations 10, 15 and 18, the performance metrics are the function of $\upsilon(x)$. To find the closed-form of the performance matrices, the closed-form expression of $\upsilon(x)$ should be derived first.

Theorem 4.1: The closed-form expression of $\upsilon(x)$ is given by

$$\upsilon(x)=\begin{cases}\frac{\beta x}{2}\sum_{m=1}^{M}(-1)^{m-1}\left(\begin{array}{c}\left(\frac{\tau_x}{\alpha}\right)^{2/\beta}{}_1F_1\left(1,1+\frac{2}{\beta},(1-m)\tau_x\right)\\ -r^2x^{1-m}{}_1F_1\left(1,1+\frac{2}{\beta},(1-m)\tau_1\right)\end{array}\right) & for \quad x>1\\ \quad+\frac{x}{\beta}\sum_{m=1}^{M+1}(-1)^{m-1}(\alpha m)^{-2/\beta}U\left(1-\frac{2}{\beta},1-\frac{2}{\beta},m\tau_x\right) & \\ \frac{x}{\beta}\sum_{m=1}^{M+1}(-1)^{m-1}x^m(\alpha m)^{-2/\beta}U\left(1-\frac{2}{\beta},1-\frac{2}{\beta},m\tau_1\right) & for \qquad x<1\end{cases} \tag{23}$$

in which

- $\tau_x=\alpha r^\beta+\log(x)$ and $\tau_1=\alpha r^\beta$.
- ${}_1F_1(.,.,.)$ is confluent hypergeometric function of the first kind
- $U(.,.,.)$ is confluent hypergeometric function of the second kind

A. When $2/\beta$ is an integer

When $2/\beta$ is an integer, $\upsilon(x)$ can be obtained by

$$\upsilon(x)=\begin{cases}\left(\begin{array}{c}x\frac{\beta}{2}\frac{1}{(2/\beta)!}\sum_{\omega=1}^{2/\beta}\left(\begin{array}{c}\frac{\tau_x^{2/\beta}}{\alpha^{2/\beta}}\tau_x^{-\omega}\\ -r^2\tau_1^{-\omega}\end{array}\right)\sum_{m=1}^{M}\frac{(-1)^{m-1}}{(1-m)^\omega}\\ +x\frac{(2/\beta-1)!}{\alpha^{2/\beta}}\sum_{\omega=1}^{2/\beta}\frac{\tau_x^{\omega-1}}{(\omega-1)!}\sum_{m=1}^{M+1}\frac{(-1)^{m-1}}{m^{2/\beta-\omega+1}}\end{array}\right) & for \qquad x>1\\ x\frac{(2/\beta-1)!}{\alpha^{2/\beta}}\sum_{\omega=1}^{2/\beta}\frac{\tau_1^{\omega}}{(\omega-1)!}\sum_{m=1}^{M+1}\frac{(-x)^m}{(m+1)^{2/\beta-\omega+1}} & for \qquad x<1\end{cases} \tag{24}$$

Proof: See Appendix B □

Lemma 4.2: The association probability of user in Group n in Equation 10 and the coverage probability of the typical user in Equation 16 can be expressed by the flowing approximated closed-forms

$$\mathcal{P}_A=\sum_{m=1}^{M_G}\omega_j\left[\zeta\left(T_{n-1},0,r=\sqrt{\frac{t_i}{\pi\lambda}}\right)-\zeta\left(T_n,0,r=\sqrt{\frac{t_i}{\pi\lambda}}\right)\right] \tag{25}$$

$$\mathcal{P}_n=\frac{\sum_{m=1}^{M_G}\omega_j\left[\zeta(T_{n-1},\hat{T},r)-\zeta(T_n,\hat{T},r=\sqrt{\frac{t_i}{\pi\lambda_n}})\right]}{\sum_{m=1}^{M_G}\omega_j\left[\zeta(T_{n-1},0,r=\sqrt{\frac{t_i}{\pi\lambda_n}})-\zeta(T_n,0,r=\sqrt{\frac{t_i}{\pi\lambda_n}})\right]} \tag{26}$$

$$\mathcal{P}(\hat{T})=\sum_{n=1}^{N}\sum_{m=1}^{N_G}\omega_j\left[\zeta\left(T_{n-1},\hat{T},r=\sqrt{\frac{t_i}{\pi\lambda_n}}\right)-\zeta\left(T_n,\hat{T},r=\sqrt{\frac{t_i}{\pi\lambda_n}}\right)\right] \tag{27}$$

where N_G are the degree of the Laguerre polynomial, t_i and w_i are the i-th node and weight of the quadrature.

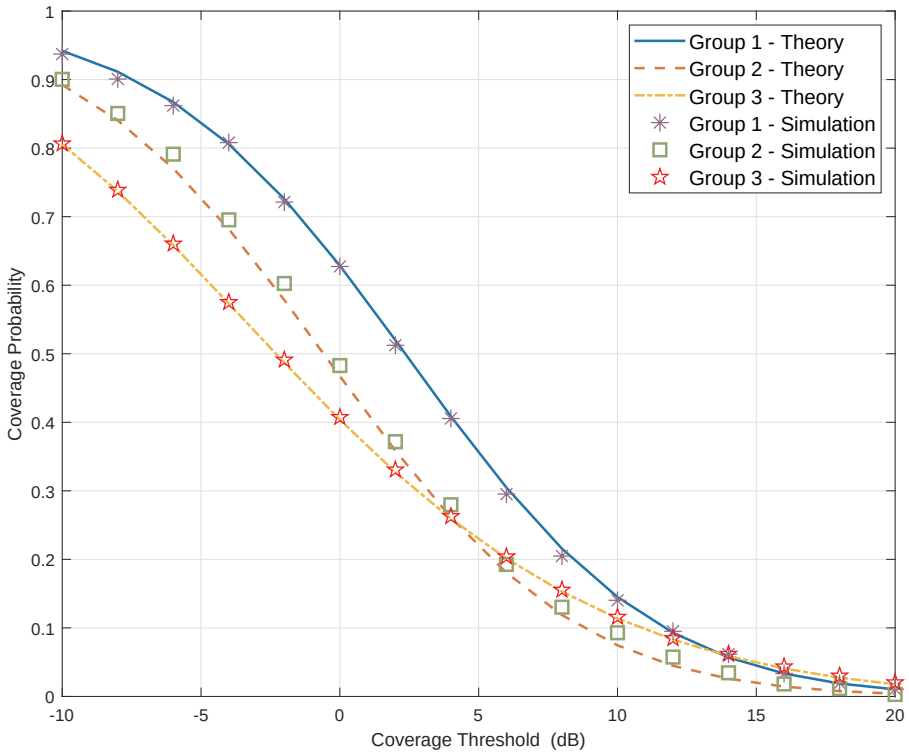

Fig. 1. Coverage probability of user groups

Proof: The desired results are obtained by using a change of variable $y = \pi\lambda r^2$, $y = \pi\lambda_n r^2$ and utilizing the Gauss - Laguerre [33] which states that $\int_0^\infty f(t)e^{-t} \approx \sum_{i=1}^{N_{GL}} \omega_i f(t_i)$ □

V. Simulation and Performance Analysis

A. Theoretical Validation

In this section, we utilize Monte - Carlo simulation to verify the analytical results. The tunable parameter of the stretch path loss model are selected as $\beta = 2/3$ and $\alpha = 0.3$. The number of users groups is $N = 3$ and four thresholds are adopted as $T_0 = -\infty, T_1 = -15, T_2 = -13, T_3 = \infty$ dB. According to 3GPP recommendation [34], the power ratio between group varies from 2 to 20. Thus, the serving powers of user groups are selected as $P_1 = 10P_3, P_2 = 5P_3$. The density of BSs is assumed at $\lambda = 30\ BS/km^2$. As shown in Figure 1, the theoretical curves visually match with the Monte Carlo simulation ones, which can confirm the accuracy of the analytical results.

With the selection of SINR thresholds, the users in Group 1, 2 and 3 are users with downlink SINR on the control channel during establishment phase in ranges (-$\infty, -15$), $(-15, -13)$, and $(-13, \infty)$ dB respectively. However, Figure 1 indicates that the typical user during communication phase in Group 1

outperform other in Group 2and Group 3 . For example, when coverage threshold $\hat{T} = 0$ dB, the coverage probability of the typical user in Group 1 P_1= 0.7112 which is 1.256 and 1.448 times greater than others in Group 2 and Group 3, respectively. This phenomenon can be explained as follows

- During the communication phase, all users experience the same statistical interference power.
- The serving power of the users in Group 1 is 10 and 5 times greater than those in Group 2 and 3 respectively

Therefore, the users in Group 1 can experience higher SINR and consequently better coverage probability.

B. Effects of SNR and density of BSs

In Figure 2, we examine the effects of SNR and the density of BSs on the coverage probability of the typical user in which SNR is defined as $SNR = P/\sigma^2$. There are two interesting findings in this figure that contradicts to other related works in the literature.

1) Finding 1: The user coverage probability increases to the peak before passing a decline when the density of BSs λ increases.
2) Finding 2: At high values of λ, increasing the serving power of a user may results in the decline of its performance.

Regarding to Finding 1, the authors in [15] stated that the user coverage probability exponentially reduces when λ increases. In [15], the authors assumed that $SNR \approx +\infty$. Hence, the effect of SNR on the network performance was not considered.

In the case of SNR is limited, the downlink SINR from Equation 13 is re-written as follows

$$SINR_n(r) = \frac{gL_r}{I/P_n + 1/SNR} \tag{28}$$

When λ is a small number such as $\lambda < 60$ in the case of $SNR = 20$ dB, an increase in λ leads to the growth of serving power, and interfering power which is still small compared to $1/SNR$. Thus, the denominator of Equation 28 increases at a higher rate than the numerator. Consequently the received SINR and user coverage probability increases in this case. Specifically, when λ increases from 10 to 40, the user coverage probability rises by 63% from 0.4968 to 0.8905. In contrast, when λ is large enough, an increment in interfering power obtained when λ increases greater than $1/SNR$. Thus, both the received SINR and user coverage probability experience declines.

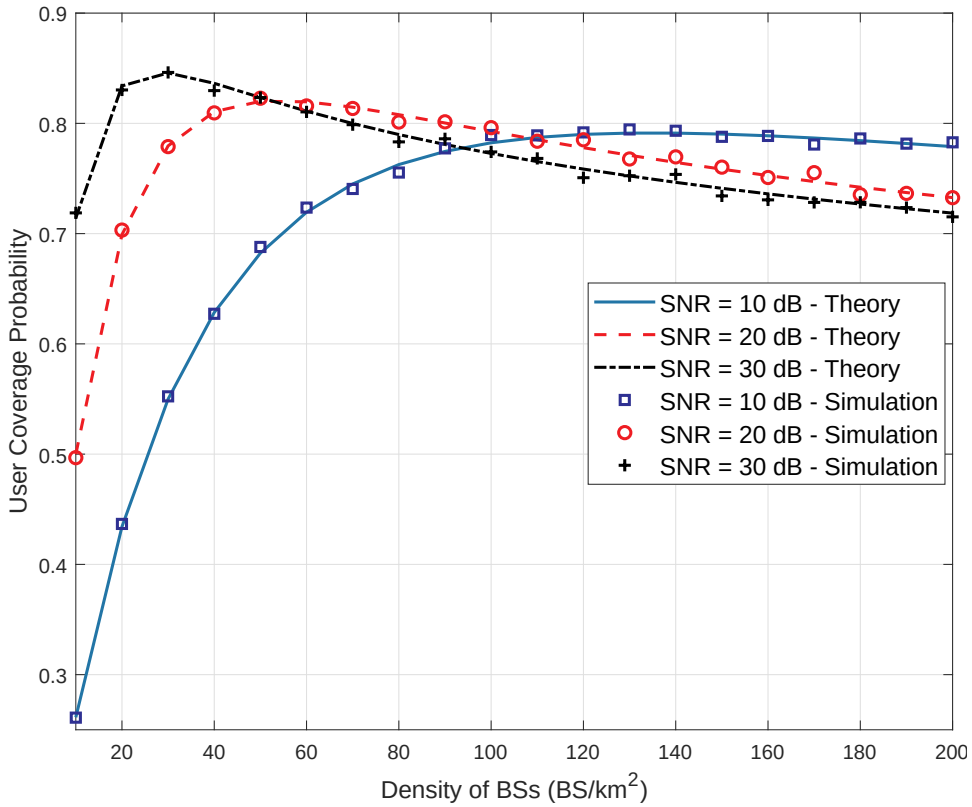

Fig. 2. Effects of SNR and density of BSs on user performance

Regarding the Finding 2, most of the works in the literature stated that when transmit power increases, the user performance reaches to a peak and keeps constant. However, in the case of UDNs utilizing FFR, an increase in the transmission power lead to an improvement to the received SINR during the establishment phase. Thus, some users will be pushed from lower groups with high serving powers such as Group 1,2 to higher groups such as Group 2,3 with low serving powers. When λ is a small number, the interfering power is relatively smaller than $1/SNR$. Thus, an increase in SNR leads to a significant decline in $1/SNR$ and consequently the interfering power + $1/SINR$. Thus, the user coverage probability increases with SNR when λ is relatively small. In contrast, the interfering power is significantly greater than $1/SNR$ if λ is large enough. Therefore, the positive effects of SNR on the user coverage probability reduces with SNR. This may result in a decline in user coverage probability when SNR increases. Take $\lambda = 180$ for example, the user coverage probability is 0.7863 at SNR = 10 dB which is 7.6% greater than that at SNR=30dB. Generally, this finding can state that if an increases in the density of BSs is compulsory, please reduce their transmission power.

C. Effects of number of user groups

In this section, we compare the user coverage probability for two cases: $N = 2$ and $N = 3$. The total power of a BS is set the same for both cases. Thus, these cases have different user classification strategies which are represented through the SINR thresholds. The analytical parameters are selected as the following table.

TABLE I
COMPARISION PARAMETERS IN CASES OF $N = 2$ AND $N = 3$

	Threshold (dB)	Power	P_{An}
N=2	$(-\infty, -2.5, \infty)$	$10P, P$	$0.7108, 0.2892$
N=3	$(-\infty, -7.5, 8.5, \infty)$	$10P, 5P, P$	$0.4659, 0.5165, 0.0176$

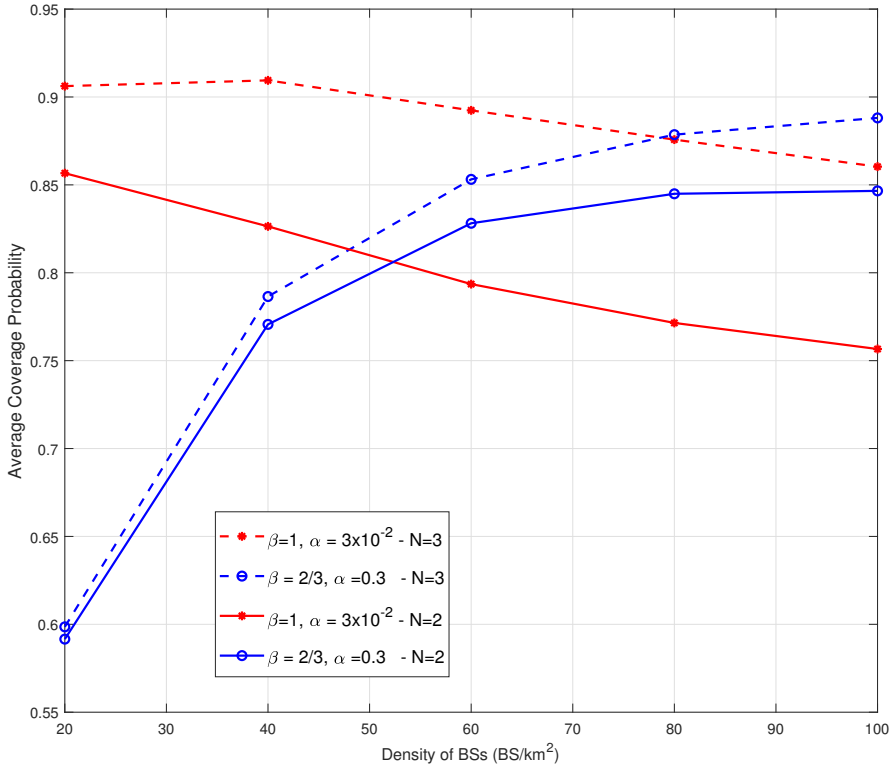

Fig. 3. Effects of number of user groups on user performance

Due to the fast attenuation of mmWave, the received SINR on the downlink of the typical user varies in a large range. Thus, use of a specific power level may not efficiently improve the performance of users. For example in the case of $N = 2$ with SINR threshold $T_1 = -2.5$dB, three are some users with $SINR << -2.5$ dB. These users requires a significantly higher power to achieve acceptable performance. Thus, the serving power $10P$ is a suitable choice for these users. However, there exists users with $SINR \approx -2.5$ dB. Use of a high power level such as $10P$ may bring negative effects to user performance as analysis in

Section V-C. Therefore, the system with a higher number of user groups can achieve better performance than others.

As seen from Figure 3, the system with three user groups ($N = 3$) outperform other with two user groups ($N = 2$), especially when the density of BSs λ is at high values. For example, when $\lambda = 80$ BS/km^2, the coverage of the typical user in the case of $N = 3$ is at 0.8786 which is 13.9% higher that corresponding value in the case of $N = 2$

VI. Conclusion

This paper modeled a UDNs network system utilizing FFR in which the associated users of each BS are classified into N groups. By which each group is served by a predetermined power level. Throughout the mathematical transformation, the user coverage probability was derived. The paper introduced a simple approach to obtain user coverage probability in the case of a general path loss model and approximated form in the case of stretch path loss model. Through the analytical and simulation results, two interesting statements were found: *(i)* the user coverage probability reach a peak before passing a decline when the density of BSs increases, *(ii)* an increase in transmission power may result in a decline in user coverage probability. The paper also stated that an increase in number of user groups can improve the user performance without additional requirement of BS transmission power, particularly the user coverage probability increase 13.9% when the number of user groups rises from 2 to 3.

VII. Acknowledgement

This work has been supported by Vietnam National University, Hanoi (VNU), under Project No. QG.20.52

Appendix A
Proof of Theorem 3.1

Ihe coverage probability of the user at a distance r from its serving BS which is defined in Equation 14 can be re-written as follows

$$\begin{aligned}\mathcal{P}_n^{SINR} &= \mathbb{P}\left(SINR_n(r) > \hat{T} \middle| T_{n-1} < SINR^{(o)}(r) < T_n\right) \\ &= \frac{\mathbb{P}\left(SINR_n(r) > \hat{T}, T_{n-1} < SINR^{(o)}(r) < T_n\right)}{\mathbb{P}\left(T_{n-1} < SINR^{(o)}(r) < T_n\right)}\end{aligned} \tag{29}$$

The numerator of Equation 29 is computed as the following steps

$$\begin{aligned}
&\mathbb{P}\left(SINR_n(r) > \hat{T}, T_{n-1} < SINR^{(o)}(r) < T_n\right) \\
&= \mathbb{P}\left(\frac{P_n g L(r)}{I+\sigma^2} > \hat{T}, T_{n-1} < \frac{g^{(o)} L(r)}{I_o + 1/\gamma} < T_n\right) \\
&= \mathbb{P}\left(g > \hat{T}\frac{I+\sigma^2}{P_n g L(r)}, \frac{T_{n-1}\left(I_o+\sigma^2\right)}{P_N L(r)} < g^{(o)} < \frac{T_n\left(I_o+\sigma^2\right)}{P_N L(r)}\right)
\end{aligned} \tag{30}$$

in which I_o and I are defined in Equations 4 and 12. Since g and $g^{(o)}$ are exponential random variables with CDF $f(x) = \exp(-x)$, the probability above can be re-written as follows

$$\mathbb{E}\left[\hat{s}\prod_{k=1}^{N}\prod_{j\in\theta_k}\exp\left(-\hat{T}\frac{P_k g_j L(r_j)}{P_n L(r)}\right)\left(\begin{array}{c} s_{n-1}\prod_{j\in\theta}\exp\left(-\frac{T_{n-1}g_j^{(o)}L(r_j)}{L(r)}\right) \\ -s_n\prod_{j\in\theta}\exp\left(-\frac{T_n g_j^{(o)}L(r_j)}{L(r)}\right)\end{array}\right)\right] \tag{31}$$

in which $\hat{s} = \exp\left(-\frac{1}{L(r)}\frac{\hat{T}}{\gamma_n}\right)$ and $s_n = \exp\left(-\frac{1}{L(r)}\frac{T_n}{\gamma_N}\right)$

Taking the expectation with respect to random variable r whose PDF is given by Equation 1

$$2\pi\lambda\int_0^\infty \mathbb{E}\left[\begin{array}{c}\hat{s}\prod_{k=1}^{N}\prod_{j\in\theta_k}\exp\left(-\hat{T}\frac{P_k L(r_j)}{P_n L(r)}g_j\right) \\ \times\left(\begin{array}{c} s_n\prod_{j\in\theta}\exp\left(-T_n\frac{L(r_j)}{L(r)}g_j^{(o)}\right) \\ -s_{n-1}\prod_{j\in\theta}\exp\left(-T_{n-1}\frac{L(r_j)}{L(r)}g_j^{(o)}\right)\end{array}\right)\end{array}\right]\exp\left(-\pi\lambda r^2\right)dr \tag{32}$$

The expectation in Equation 32 can be expressed as the difference of two expectations in which the second one, denoted by $\zeta(T_n, \hat{T}, r)$ can be evaluated as follows

$$\begin{aligned}
\zeta(T_n,\hat{T},r) &= \mathbb{E}\left[\hat{s}s_n\prod_{k=1}^{N}\prod_{j\in\theta_k}\frac{1}{1+\hat{T}\frac{P_k L_{r_j}}{P_n L_r}}\prod_{j\in\theta}\frac{1}{1+\frac{T_{n-1}L_{r_j}}{L_r}}\right] \\
&= \hat{s}s_n\prod_{k=1}^{N}\mathbb{E}_{\theta_k}\left[\prod_{j\in\theta_k}\frac{1}{1+\hat{T}\frac{P_k L_{r_j}}{P_n L_r}}\frac{1}{1+\frac{T_n L_{r_j}}{L_r}}\right] \\
&= \hat{s}s_n\prod_{k=1}^{N}\exp\left[-2\pi\lambda_k\int_r^\infty\left(1-\frac{1}{1+\hat{T}\frac{\gamma_k L_{r_j}}{\gamma_n L_r}}\frac{1}{1+T_n\frac{L_{r_j}}{L_r}}\right)r_j dr_j\right] \\
&= \hat{s}s_n\prod_{k=1}^{N}\exp\left[-\frac{2\pi\lambda_k}{\hat{T}\frac{\gamma_k)}{\gamma_n}-T_n}\int_r^\infty\left[\hat{T}\frac{\gamma_k L_{r_j}}{\gamma_n L_r}\frac{1}{1+\hat{T}\frac{\gamma_k L_{r_j}}{\gamma_n L_r}}-T_n^2\frac{L_{r_j}}{L_r}\frac{1}{1+T_n\frac{L_{r_j}}{L_r}}\right]r_j dr_j\right]
\end{aligned} \tag{33}$$

in which Equation 33 is obtained by assuming that $\hat{T}\frac{\gamma_k L_{r_j}}{\gamma_n L_r} \neq T_n$

These integrals in Equation 33 can be simplified using the application of Taylor series that states [35]

$$\frac{1}{x+1} = \begin{cases} \sum_{m=1}^{M} (-1)^{m-1} x^{-m} & for \quad x > 1 \\ \sum_{m=0}^{M} (-1)^{m} x^{m} & for \quad x < 1 \end{cases}, \tag{34}$$

Thus the second integral, denoted by $\upsilon(T_n)$, can be expanded as follows

- If $T_n > 1$, then $T_n \frac{L_{r_j}}{L_r} > 1$ when $r = r_j$

$$\upsilon(T_n) = L_r^{m-1} T_n^{2-m} \sum_{m=1}^{M} (-1)^{m-1} \int_{r}^{L_{\frac{L_r}{T}}^{-1}} r_j L_{r_j}^{1-m} dr_j + T_n^{m+2} L_r^{-1-m} \sum_{m=0}^{M} (-1)^{m} \int_{L_{\frac{L_r}{T}}^{-1}}^{\infty} r_j L_{r_j}^{m} dr_j \tag{35}$$

- If $T_n < 1$, then $T_n \frac{L_{r_j}}{L_r} < 1$ when $r = r_j$

$$\upsilon(T_n) = T_n^{m+2} L_r^{-1-m} \sum_{m=0}^{M} (-1)^{m} \int_{r}^{\infty} L_{r_j}^{m+1} r_j dr_j \tag{36}$$

Similarly, the first integral in Equation 33 can be expressed as $\upsilon\left(\hat{T}\frac{\gamma_k}{\gamma_n}\right)$. Hence $\zeta(T_n, \hat{T}, r)$ can be re-written as follows

$$\zeta(T_n, \hat{T}, r) = \hat{s} s_n \prod_{k=1}^{N} \exp\left[-\frac{2\pi\lambda_k}{\hat{T}\frac{\gamma_k}{\gamma_n} - T_n} \left(\upsilon\left(\hat{T}\frac{\gamma_k}{\gamma_n}\right) - \upsilon(T_n) \right) \right] \tag{37}$$

Similarity, the first expectation in Equation 32 is $\zeta(T_{n-1}, \hat{T}, r)$ which is obtained by replacing $\hat{T}$ in Equation 37 by $\hat{T}\frac{\gamma_k)}{\gamma_n}$.

The numerator can be obtained by utilizing above approach for $\hat{T} = 0$. Hence, the numerator is given by

$$2\pi\lambda \int_{0}^{\infty} \left[s_{n-1} \exp\left[-2\pi\lambda \frac{\upsilon(T_{n-1})}{T_{n-1}} \right] - s_n \exp\left[-2\pi\lambda \frac{\upsilon(T_n)}{T_n} \right] \right] f(r) dr \tag{38}$$

Consequently, the coverage probability $\mathcal{P}_n$ is obtained by

$$\mathcal{P}_n = \frac{2\pi\lambda \int_{0}^{\infty} \left[\begin{pmatrix} \hat{s} s_{n-1} \prod_{k=1}^{N} \exp\left[-\frac{2\pi\lambda_k}{\hat{T}\frac{\gamma_k}{\gamma_n} - T_{n-1}} \left(\upsilon\left(\hat{T}\frac{\gamma_k}{\gamma_n}\right) - \upsilon(T_{n-1}) \right) \right] \\ -\hat{s} s_n \prod_{k=1}^{N} \exp\left[-\frac{2\pi\lambda_k}{\hat{T}\frac{\gamma_k}{\gamma_n} - T_n} \left(\upsilon\left(\hat{T}\frac{\gamma_k}{\gamma_n}\right) - \upsilon(T_n) \right) \right] \end{pmatrix} \right] f(r) dr}{2\pi\lambda \int_{0}^{\infty} \left[s_{n-1} \exp\left[-2\pi\lambda \frac{\upsilon(T_{n-1})}{T_{n-1}} \right] - s_n \exp\left[-2\pi\lambda \frac{\upsilon(T_n)}{T_n} \right] \right] f(r) dr} \tag{39}$$

The Theorem 3.1 has been proved.

APPENDIX B

Substituting $L_{r_j} = \exp\left(\alpha r_j^{\beta}\right)$, there integrals of $v(x)$ can be computed as follows

1) The first integral

$$\begin{aligned}
&\int_{r}^{L^{-1}_{\frac{L_r}{x}}} r_j L_{r_j}^{1-m} dr_j \\
&= \int_{r}^{\left(r^{\beta}+\frac{log(x)}{\alpha}\right)^{1/\beta}} r_j \exp\left(-\alpha(1-m)r^{\beta}\right) dr_j \\
&= \frac{1}{\beta}\int_{0}^{r^{\beta}+\frac{log(x)}{\alpha}} u^{2/\beta-1}\exp\left(-\alpha(1-m)u\right) du - \frac{1}{\beta}\int_{0}^{r^{\beta}} u^{2/\beta-1}\exp\left(-\alpha(1-m)u\right) du \qquad (40)\\
&= \frac{1}{2\alpha^{2/\beta}}\tau_x^{2/\beta}{}_1F_1\left(\frac{2}{\beta}, 1+\frac{2}{\beta}, (m-1)\tau_x\right) - \frac{r^2}{2}{}_1F_1\left(\frac{2}{\beta}, 1+\frac{2}{\beta}, (m-1)\tau_1\right) \qquad (41)
\end{aligned}$$

in which Equation 40 follows transformation of variable $u = r^{\beta}$, Equation 41 follows [36, p.348] Using the properties of confluent hypergeometric function of the first kind, ${}_1F_1(a,b,z) = e^z{}_1F_1(b-a,b,-z)$, then

$$\begin{aligned}
&\frac{1}{2\alpha^{2/\beta}}\tau_x^{2/\beta}\exp\left((m-1)\tau_x\right){}_1F_1\left(1, 1+\frac{2}{\beta}, (1-m)\tau_x\right) \\
&\quad - \frac{1}{2\alpha^{2/\beta}}\tau_1^{2/\beta}\exp\left((m-1)\tau_1\right){}_1F_1\left(1, 1+\frac{2}{\beta}, (1-m)\tau_1\right) \qquad (42)
\end{aligned}$$

- When $2/\beta$ is an integer, the confluent hypergeometric function of the first kind ${}_1F_1$ is obtained by [35, p.324]

$$ {}_1F_1\left(1, 1+\frac{2}{\beta}, (1-m)\tau_1\right) = \sum_{\omega=1}^{2/\beta} \frac{1}{(2/\beta)!}\left((1-m)\tau_1\right)^{-\omega} \qquad (43)$$

2) The second integral

$$\begin{aligned}
\int_{L^{-1}_{\frac{L_r}{x}}}^{\infty} r_j L_{r_j}^{m+1} dr_j &= \int_{\left(r^{\beta}+\frac{log(x)}{\alpha}\right)^{1/\beta}}^{\infty} r_j \exp(-\alpha(m+1)r_j^{\beta}) dr_j \\
&= \frac{1}{\beta}\int_{r^{\beta}+\frac{log(x)}{\alpha}}^{\infty} u^{2/\beta-1}\exp(-\alpha(m+1)u) du \\
&= \frac{1}{\beta}(\alpha(m+1))^{-2/\beta}\Gamma\left(\frac{2}{\beta}, (m+1)\tau_x\right) \qquad (44)\\
&= \frac{1}{\beta}(\alpha(m+1))^{-2/\beta}\exp\left(-(m+1)\tau_x\right) U\left(1-\frac{2}{\beta}, 1-\frac{2}{\beta}, (m+1)\tau_x\right) \qquad (45)
\end{aligned}$$

where Equation 44 is obtained by following [36, p.346] and $\Gamma(x,y)$ is the upper incomplete gamma function; Equation 45 follows the relationship between the incomplete gamma function and the

confluent hypergeometric function of the second kind U [35].

- When $2/\beta$ is an integer, the incomplete gamma function can be computed as $\Gamma(n+1,z) = n!e^{-z}\sum_{k=1}^{n+1}\frac{z^{k-1}}{(k-1)!}$. Hence, the integral becomes

$$\int_{L^{-1}_{\frac{L_T}{x}}}^{\infty} r_j L^m_{r_j} dr_j = \frac{\beta\,(2/\beta-1)!x^{-(m+1)}}{(\alpha(m+1))^{2/\beta}}\exp\left(-(m+1)\alpha r^{\beta}\right)\sum_{u=1}^{2/\beta}\frac{(m+1)^{u-1}\tau_x^u}{(u-1)!} \tag{46}$$

  in which Equation 46 follows the binomial expansion.

  Substituting Equations 42 and 45 into Equation 9 and change the sum index from $(0, M)$ to $(1, M+1)$, we get the first case ($x > 0$) of Equation 23. The result for $x > 0$ in Equation 24 is obtained by substituting Equations 42 and 46 into Equation 9.

3) The third integral for $x < 0$ can be computed in the same manner for the second one, i.e. by letting $x = 1$.

ACKNOWLEDGMENT

REFERENCES

[1] Cisco, "Cisco visual networking index: Global mobile data traffic forecast update, 2015 ? 2020," 2016.

[2] M. Agiwal, A. Roy, and N. Saxena, "Next generation 5g wireless networks: A comprehensive survey," *IEEE Communications Surveys Tutorials*, vol. 18, no. 3, pp. 1617–1655, thirdquarter 2016.

[3] J. G. Andrews, S. Buzzi, W. Choi, S. V. Hanly, A. Lozano, A. C. K. Soong, and J. C. Zhang, "What will 5g be?" *IEEE Journal on Selected Areas in Communications*, vol. 32, no. 6, pp. 1065–1082, 2014.

[4] W. Yu, H. Xu, H. Zhang, D. Griffith, and N. Golmie, "Ultra-dense networks: Survey of state of the art and future directions," in *2016 25th International Conference on Computer Communication and Networks (ICCCN)*, Aug 2016, pp. 1–10.

[5] M. Kamel, W. Hamouda, and A. Youssef, "Ultra-dense networks: A survey," *IEEE Communications Surveys Tutorials*, vol. 18, no. 4, pp. 2522–2545, Fourthquarter 2016.

[6] C. Galiotto, N. K. Pratas, L. Doyle, and N. Marchetti, "Effect of los/nlos propagation on 5g ultra-dense networks," *Computer Networks*, vol. 120, pp. 126 – 140, 2017. [Online]. Available: http://www.sciencedirect.com/science/article/pii/S1389128617301536

[7] M. Ding, P. Wang, D. Lopez-Perez, G. Mao, and Z. Lin, "Performance impact of los and nlos transmissions in dense cellular networks," *IEEE Transactions on Wireless Communications*, vol. 15, no. 3, pp. 2365–2380, March 2016.

[8] I. Atzeni, J. Arnau, and M. Kountouris, "Downlink cellular network analysis with los/nlos propagation and elevated base stations," *IEEE Transactions on Wireless Communications*, vol. 17, no. 1, pp. 142–156, 2018.

[9] K. Cho, J. Lee, and C. G. Kang, "Low-complexity coverage analysis of downlink cellular network for combined los and nlos propagation," *IEEE Communications Letters*, vol. 23, no. 1, pp. 160–163, 2019.

[10] M. Ding, D. Lopez-Perez, Y. Chen, G. Mao, Z. Lin, and A. Zomaya, "Udn: A holistic analysis of multi-piece path loss, antenna heights, finite users and bs idle modes," *IEEE Transactions on Mobile Computing*, pp. 1–1, 2019.

[11] M. Ding and D. Lopez Perez, "Please lower small cell antenna heights in 5g," in *2016 IEEE Global Communications Conference (GLOBECOM)*, 2016, pp. 1–6.

[12] H. Cho, C. Liu, J. Lee, T. Noh, and T. Q. S. Quek, "Impact of elevated base stations on the ultra-dense networks," *IEEE Communications Letters*, vol. 22, no. 6, pp. 1268–1271, 2018.

[13] M. Franceschetti, J. Bruck, and L. J. Schulman, "A random walk model of wave propagation," *IEEE Transactions on Antennas and Propagation*, vol. 52, no. 5, pp. 1304–1317, 2004.

[14] D. Ramasamy, R. Ganti, and U. Madhow, "On the capacity of picocellular networks," in *2013 IEEE International Symposium on Information Theory*, 2013, pp. 241–245.

[15] A. AlAmmouri, J. G. Andrews, and F. Baccelli, "Sinr and throughput of dense cellular networks with stretched exponential path loss," *IEEE Transactions on Wireless Communications*, vol. 17, no. 2, pp. 1147–1160, Feb 2018.

[16] L. Yang and W. Zhang, *Interference Coordination for 5G Cellular Networks*. Springer International Publishing, 2015.

[17] B. Soret, A. D. Domenico, S. Bazzi, N. H. Mahmood, and K. I. Pedersen, "Interference coordination for 5g new radio," *IEEE Wireless Communications*, vol. 25, no. 3, pp. 131–137, 2018.

[18] B. Singh, O. Tirkkonen, Z. Li, and M. A. Uusitalo, "Interference coordination in ultra-reliable and low latency communication networks," in *2018 European Conference on Networks and Communications (EuCNC)*, 2018, pp. 1–255.

[19] L. Su, C. Yang, and C. I, "Energy and spectral efficient frequency reuse of ultra dense networks," *IEEE Transactions on Wireless Communications*, vol. 15, no. 8, pp. 5384–5398, 2016.

[20] N. Al-Falahy and O. Y. K. Alani, "Network capacity optimisation in millimetre wave band using fractional frequency reuse," *IEEE Access*, vol. 6, pp. 10 924–10 932, 2018.

[21] C. Zheng, L. Liu, and H. Zhang, "Cross-tier cooperation load-adapting interference management in ultra-dense networks," *IET Communications*, vol. 13, no. 14, pp. 2069–2077, 2019.

[22] J. Liu, M. Sheng, L. Liu, and J. Li, "Interference management in ultra-dense networks: Challenges and approaches," *IEEE Network*, vol. 31, no. 6, pp. 70–77, 2017.

[23] T. D. Novlan, R. K. Ganti, A. Ghosh, and J. G. Andrews, "Analytical Evaluation of Fractional Frequency Reuse for OFDMA Cellular Networks," *IEEE Trans. Wireless Commun.*, vol. 10, pp. 4294–4305, 2011.

[24] S. C. Lam and K. Sandrasegaran, "Performance analysis of fractional frequency reuse in uplink random cellular networks," *Phys. Commun.*, vol. 25, no. P2, pp. 469–482, Dec. 2017. [Online]. Available: https://doi.org/10.1016/j.phycom.2017.09.008

[25] X. Liu, "Closed-form coverage probability in cellular networks with poisson point process," *IEEE Transactions on Vehicular Technology*, vol. 68, no. 8, pp. 8206–8209, 2019.

[26] O. M. A. P.-I. . M. D. R. Alexis I. Aravanis, Thanh Tu Lam, "A tractable closed form approximation of the ergodic rate in poisson cellular networks," *EURASIP Journal on Wireless Communications and Networking*, 2019.

[27] M. Kamel, W. Hamouda, and A. Youssef, "Uplink coverage and capacity analysis of mmtc in ultra-dense networks," *IEEE Transactions on Vehicular Technology*, vol. 69, no. 1, pp. 746–759, 2020.

[28] L. Cong, N. Tuan, and K. Sandrasegaran, "A general model of fractional frequency reuse: Modelling and performance analysis," *VNU Journal of Science: Computer Science and Communication Engineering*, vol. 36, no. 1, 2020.

[29] Y. Xiaobin and A. O. Fapojuwo, "Performance analysis of poisson cellular networks with lognormal shadowed Rayleigh fading," in *2014 IEEE Int. Conf. Commun. (ICC),*, Conference Proceedings, pp. 1042–1047.

[30] A. S. Hamza, S. S. Khalifa, H. S. Hamza, and K. Elsayed, "A Survey on Inter-Cell Interference Coordination Techniques in OFDMA-Based Cellular Networks," *IEEE Commun. Surveys & Tutorials*, vol. 15, no. 4, pp. 1642–1670, 2013.

[31] J. G. Andrews, F. Baccelli, and R. K. Ganti, "A tractable approach to coverage and rate in cellular networks," *IEEE Transactions on Communications*, vol. 59, no. 11, pp. 3122–3134, November 2011.

[32] S. Zhang, "Inter-cell interference coordination in indoor LTE systems," Masters Thesis, 2011.

[33] M. A. Stegun and I. A., *Handbook of Mathematical Functions with Formulas, Graphs, and Mathematical Tables*, 9th ed. Dover Publications, 1972.

[34] 3GPP TR 36.828 V11.0 , "E-UTRA Further enhancements to LTE Time Division Duplex (TDD) for Downlink-Uplink (DL-UL) interference management and traffic adaptation," June 2012.

[35] F. Olver, D. Lozier, R. Boisvert, and C. Clark, "Nist handbook of mathematical functions," 01 2010.

[36] "3 - 4 - definite integrals of elementary functions," in *Table of Integrals, Series, and Products (Seventh Edition)*, seventh edition ed., A. Jeffrey, D. Zwillinger, I. Gradshteyn, and I. Ryzhik, Eds. Boston: Academic Press, 2007, pp. 247 – 617. [Online]. Available: http://www.sciencedirect.com/science/article/pii/B9780080471112500133

Sinh Cong Lam received the Bachelor of Electronics and Telecommunication (Honours) and Master of Electronic Engineering in 2010 and 2012, respectively from University of Engineering and Technology, Vietnam National University (UET, VNUH). He obtained his Ph.D degree from University of Technology, Sydney, Australia. His research interests focus on modelling, performance analysis and optimization for 4G and 5G, stochastic geometry model for wireless communications

Xuan Nam Tran received his master of engineering (ME) in telecommunications engineering from University of Technology Sydney, Australia in 1998, and doctor of engineering in electronic engineering from The University of Electro-Communications, Japan in 2003. From November 2003 to March 2006 he was a research associate at the Information and Communication Systems Group, Department of Information and Communication Engineering, The University of Electro-Communications, Tokyo, Japan . Since April 2006 he has been with Le Quy Don Technical University. Professor Xuan Nam Tran is currently Head of Strong Research Group on Advanced Wireless Communications and Head of Office of Academic Affairs, Le Quy Don Technical University, Vietnam.